2D $m_{\gamma\gamma} \times m_{bb}$ Fit for $HH \to b\bar{b}\gamma\gamma$

Kazuki Kojima (KEK)
on behalf of the 2D fit development team

France-Japan Particle Physics Network Meeting for HEP 18 Project

Sep 28th, 2026

Higgs Mechanism in Standard Model

Spontaneous electroweak symmetry breaking is an essential feature of the Standard Model, brought by the Brout-Englert-Higgs mechanism.

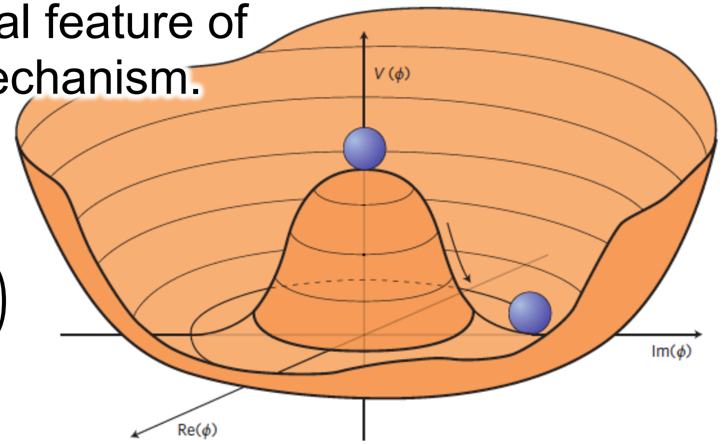

$$V(\Phi) = -\mu^2 \Phi^\dagger \Phi + \lambda \left(\Phi^\dagger \Phi\right)^2$$

electroweak symmetry breaking $\Phi \to \left(0, \dfrac{v+h}{\sqrt{2}}\right)$

$$V(h) = \frac{1}{2} m_H^2 h^2 + \lambda v h^3 + \frac{1}{4} \lambda h^4$$

$v = 246$ GeV:
Vacuum expectation value of the Higgs field

Higgs Mass

Trilinear coupling

Quartic coupling

$$\begin{aligned} \lambda &= \lambda_{HHH} \\ &= \lambda_{HHHH} \\ &= m_H^2 / 2v^2 \\ &\sim 0.13 \end{aligned}$$

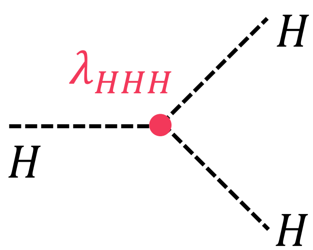

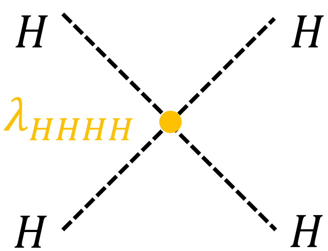

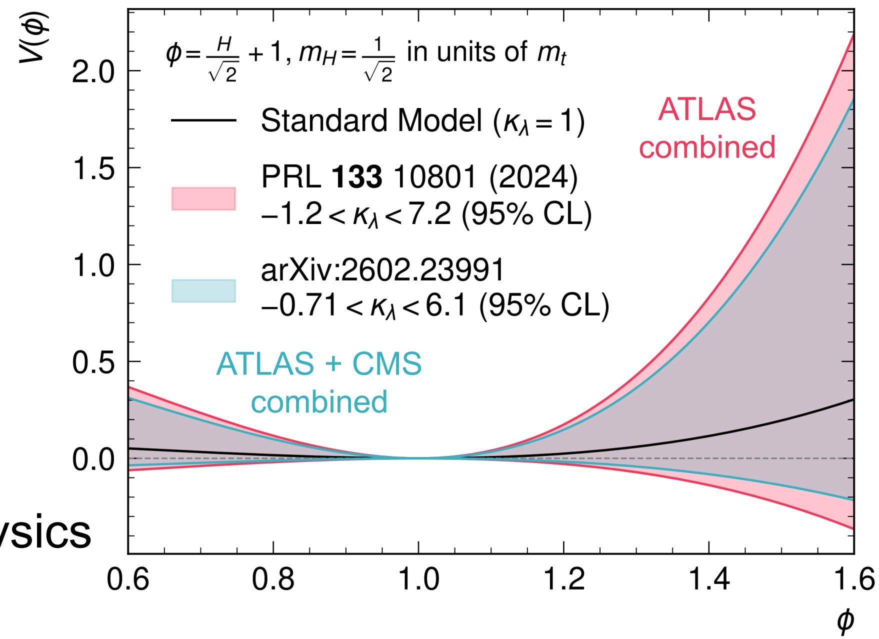

The Higgs potential could change significantly by physics beyond the Standard Model (BSM).

Determination of the Higgs potential is a probe for physics beyond the SM.

$HH \to b\bar{b}\gamma\gamma$ Searches

Non-resonant Higgs pair production searches are essential for determining the shape of the Higgs potential through the Higgs self-coupling λ measurement.

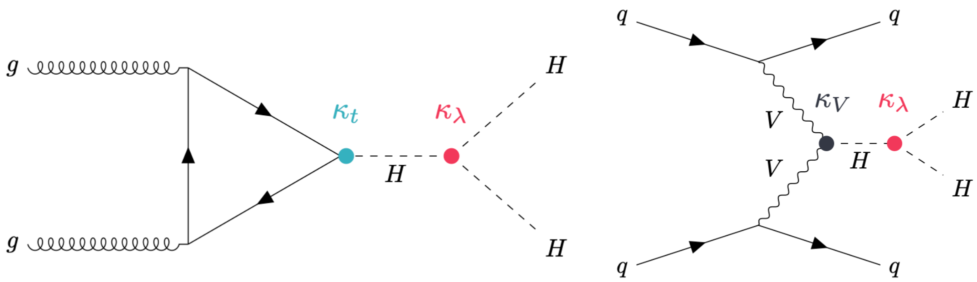

Higgs self-coupling modifier: $\kappa_\lambda = \lambda/\lambda_{\mathrm{SM}}$

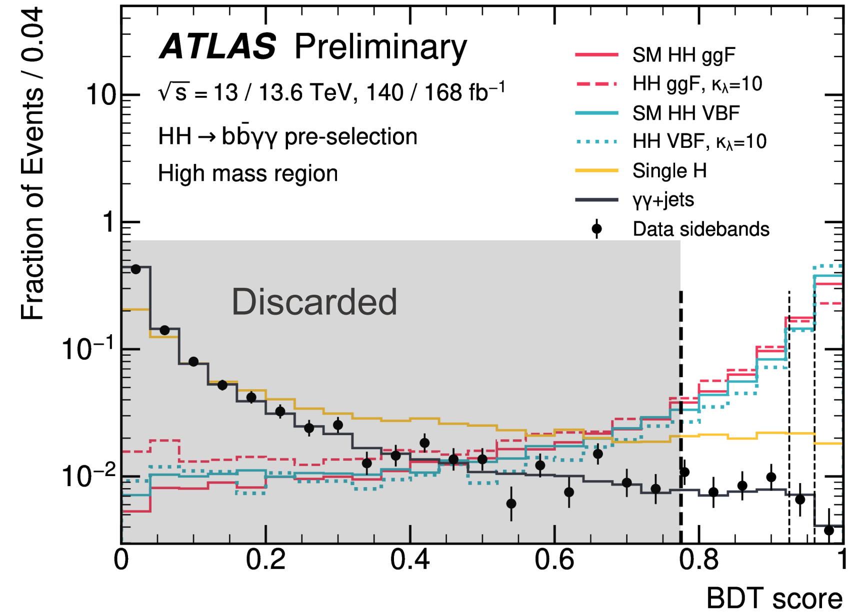

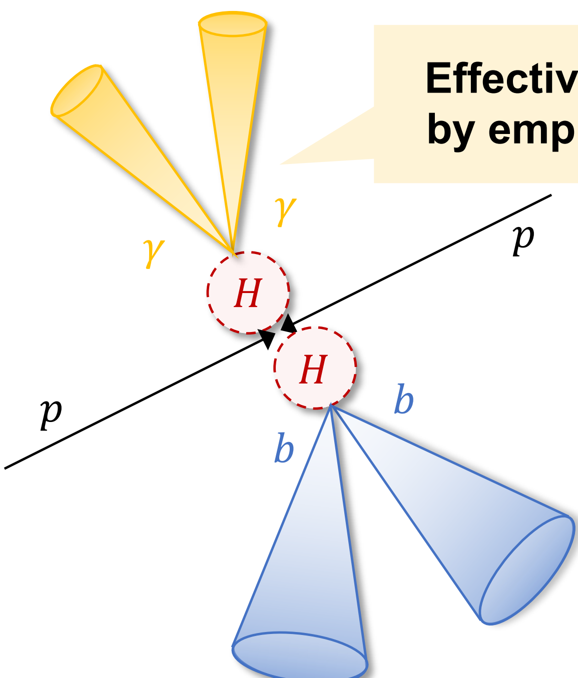

Effective background reduction by employing $m_{\gamma\gamma}$ distributions

Reconstruction → Categorisation by BDT → Simultaneous 1D $m_{\gamma\gamma}$ fits

New!

1. Transformer-based b-tagging method (GN2 85%WP)
2. m_{bb}&$m^*_{bb\gamma\gamma}$ reconstruction with kinematic fits

$HH \to b\bar{b}\gamma\gamma$ Search Results

[Phys. Lett. B **876** (2026) 140280]

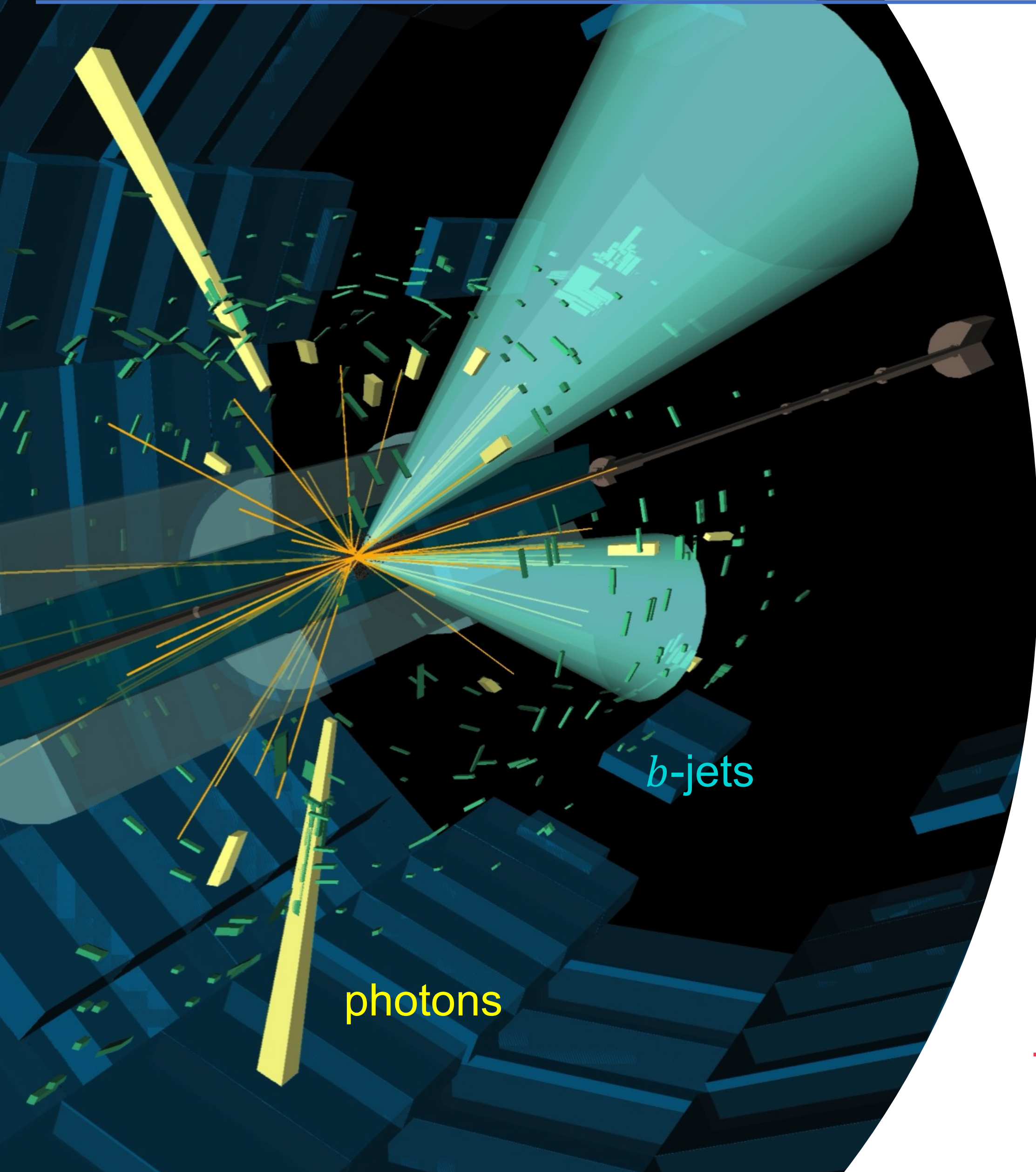

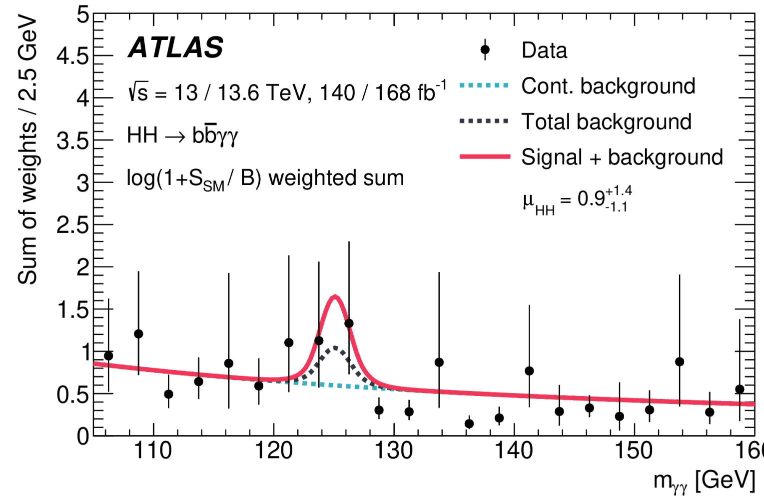

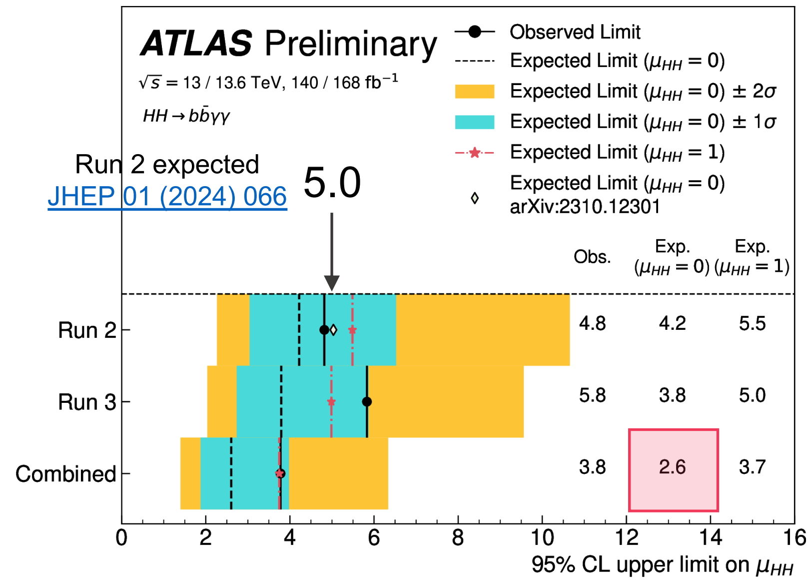

The most stringent limit as a single channel

$-1.7 < \kappa_\lambda < 6.6$ (95% CL)

2D $m_{\gamma\gamma}\times m_{bb}$ Fit for $HH \to b\bar{b}\gamma\gamma$

Extending the signal extraction method from the 1D fit on $m_{\gamma\gamma}$ to a 2D fit on $m_{\gamma\gamma}\times m_{bb}$

ATLAS $HH \to b\bar{b}\gamma\gamma$ at 308 fb^{-1}

$\mu_{HH} = 0.9\,^{+1.3}_{-1.1}\,(\mathrm{stat}) \pm 0.5\,(\mathrm{syst})$

Leading systematic uncertainty

ggF H associated with b-jets

Heavily rely on the theory expectation with $\pm 100\%$ yield uncertainty

CMS Run 3 $HH \to b\bar{b}\gamma\gamma$ at 62 fb^{-1} [link]

Expected upper limits on signal strength μ_{HH}

1D $m_{\gamma\gamma}$ fit	8.7
2D $m_{\gamma\gamma}\times m_{bb}$ fit	7.3

-16%

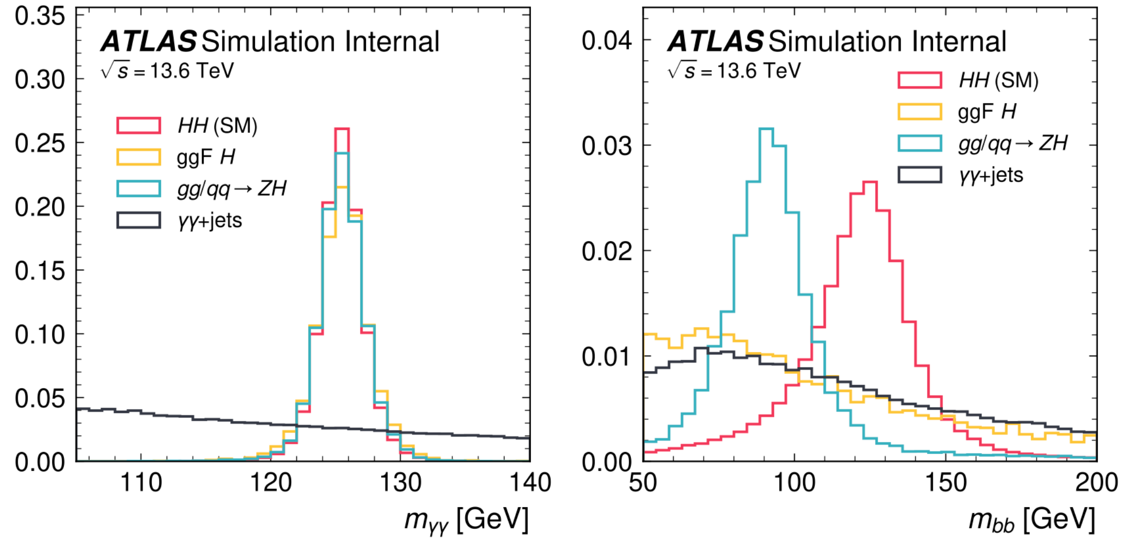

More robust single Higgs control through data-driven separation

Main challenge

1. Decorrelation against fit observables: $m_{\gamma\gamma}$ and m_{bb}
2. Spurious signal evaluation in two dimensions: $m_{\gamma\gamma}\times m_{bb}$

Developments for 2D $m_{\gamma\gamma}\times m_{bb}$ Fit

1. BDT/Transformer with m_{bb} decorrelation

2. Spurious signal study

- Spurious signal evaluation in 2D $m_{\gamma\gamma}\times m_{bb}$ fit
- Normalising flow for high-statistics $\gamma\gamma$+jets samples

3. Statistical analysis

- $m_{\gamma\gamma}\times m_{bb}$ correlations
- Categorization requirements / fit stability
- Systematic uncertainty on m_{bb} shapes

4. Framework developments

- RooFit models for a 2D double-sided Crystal Ball function
- m_{bb} modelling for single H
- Implementation to the official $HH\rightarrow b\bar{b}\gamma\gamma$ analysis framework
- Implementation to the official fit workspace generation framework

Yu Onoda
(Science Tokyo)

Yohei Yamaguchi
(KEK)

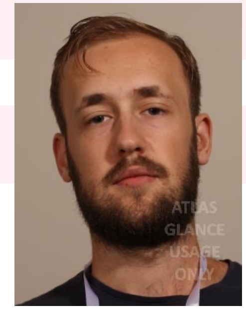

Oleksii Kurdysh
(Annecy LAPP)

Nicolò Salimbeni
(Oxford)

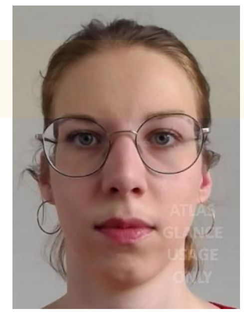

Cédrine Hügli
(DESY)

Punit Sharma
(BNL)

Elena Mazzeo
(CERN)

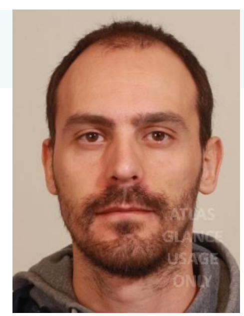

Stefano Manzoni
(CERN)

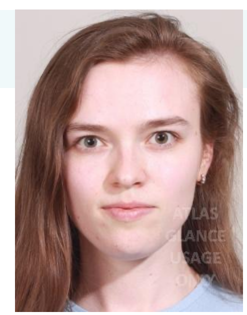

Katerina Kazakova
(Marseille CPPM)

Kazuki Kojima
(KEK)

Transformer Training with m_{bb} Decorrelation

Built transformer models through k-fold training while keeping decorrelation from m_{bb}.

Training variables

Jets $i = 1, \ldots, 10$	PCBT, η_{j_i}, ϕ_{j_i}, m_{j_i}, $m_i^{\mathrm{KF}} - m_{j_i}^{\text{before KF}}$,
Jets $i \neq 2$	$p_{\mathrm{T}}(j_i)$, $p_{\mathrm{T}}^{\mathrm{KF}}(j_i) - p_{\mathrm{T}}^{\text{before KF}}(j_i)$
Jets $i = 2$	$p_{\mathrm{T}}(j_2)/m_{bb}$, $\left(p_{\mathrm{T}}^{\mathrm{KF}}(j_i) - p_{\mathrm{T}}^{\text{before KF}}(j_i)\right)/m_{bb}$
Photons	η_{γ_1}, η_{γ_2}, ϕ_{γ_1}, ϕ_{γ_2}, $p_{\mathrm{T}}(\gamma_1)/m_{\gamma\gamma}$, $p_{\mathrm{T}}(\gamma_2)/m_{\gamma\gamma}$
MET	$E_{\mathrm{T}}^{\mathrm{miss}}$, ϕ^{miss}
Event shapes	Sphericity, planar flow, topnessPrime χ_{Wt}, p_{T} balance
VBF	m_{jj}^{VBF}, $\lvert\Delta\eta_{jj}^{\mathrm{VBF}}\rvert$
Angles	η_{bb}, ϕ_{bb}, $\eta_{bb\gamma\gamma}$, $\phi_{bb\gamma\gamma}$, $\Delta R_{\gamma\gamma}$, $\Delta R(bb, \gamma\gamma)$

Transformer

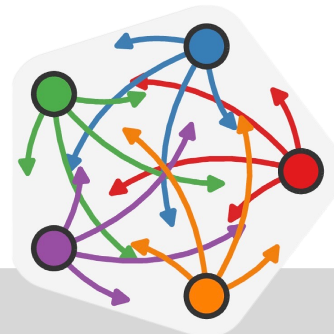

Output probabilities

HH	$p_{\mathrm{ggF}\,HH}$, $p_{\mathrm{VBF}\,HH}$
Single H	$p_{\mathrm{ggF}\,H}$, p_{ttH}, p_{ZH}, $p_{\mathrm{other}\,H}$
$\gamma\gamma$+jets	$p_{\gamma\gamma+\mathrm{jets}}$

Decorrelation scheme

1. p_{T}/m_{bb} only for sub-leading b-jet, Raw p_{T} for other b-jets
2. Training only using events at $m_{bb} \in [100, 150]$ GeV

Developed a special scheme to reduce correlation against m_{bb} → **Oleksii's talk**

Categorisation Strategy

Optimise categorization thresholds using the following discriminant:

$$D(HH) = \log\left[\frac{f_{\mathrm{ggF}\,HH}\cdot p_{\mathrm{ggF}\,HH} + f_{\mathrm{VBF}\,HH}\cdot p_{\mathrm{VBF}\,HH}}{f_{\mathrm{ggF}\,H}\cdot p_{\mathrm{ggF}\,H} + f_{ZH}\cdot p_{ZH} + f_{ttH}\cdot p_{ttH} + f_{\gamma\gamma+\mathrm{jets}}\cdot p_{\gamma\gamma+\mathrm{jets}}}\right]$$

Custom coefficients for 2D fit

$f_{\mathrm{ggF}\,HH}$	$f_{\mathrm{VBF}\,HH}$	$f_{\mathrm{ggF}\,H}$	f_{ZH}	f_{ttH}	$f_{\mathrm{other}\,H}$	$f_{\gamma\gamma+\mathrm{jets}}$
0.95	0.05	0.13	0.11	0.11	0	0.65

Optimization target

Binned counting significance

$$Z_{\mathrm{bin}} = \sqrt{2\cdot[(S+B)\cdot\log(1+S/B)-S]},\quad Z_{\mathrm{total}} = \sqrt{\sum_{\mathrm{category}}\left(\sum_{\mathrm{bin}} Z_{\mathrm{bin}}^2\right)}$$

S: HH yields ($\kappa_\lambda = 1$)

B: Single Higgs + scaled $\gamma\gamma$+ jets yields

	Bin edges
$m_{\gamma\gamma}$	$[105, 120, 122, 124, 126, 128, 130, 160]$ GeV
m_{bb}	$[50, 65, 80, 90, 100, 105, 110, 115, 120, 125, 130, 135, 140, 150, 175]$ GeV

Determine the boundaries from a median of $>$ 100 Poisson-fluctuated scans

Categorisation Results: $D(HH)$

Set boundaries for **HM** categories (b-tag 90%WP)

- 3 categories for Run 2
- 3 categories for Run 3

Common boundaries

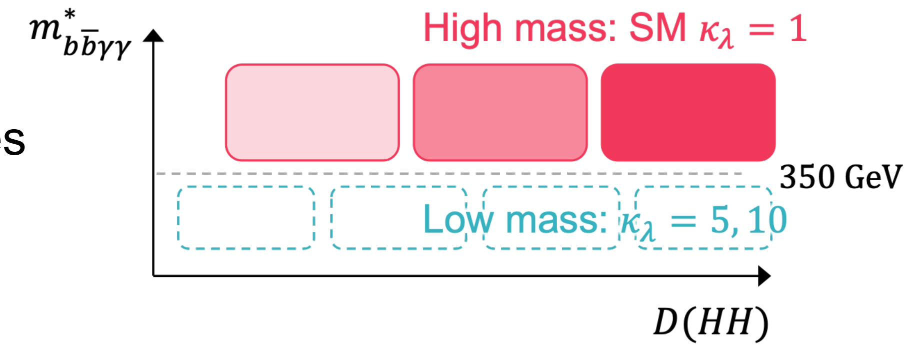

Requirements on $\gamma\gamma$+jets yields

> 11 events in $m_{\gamma\gamma} \in [105, 160]$ GeV

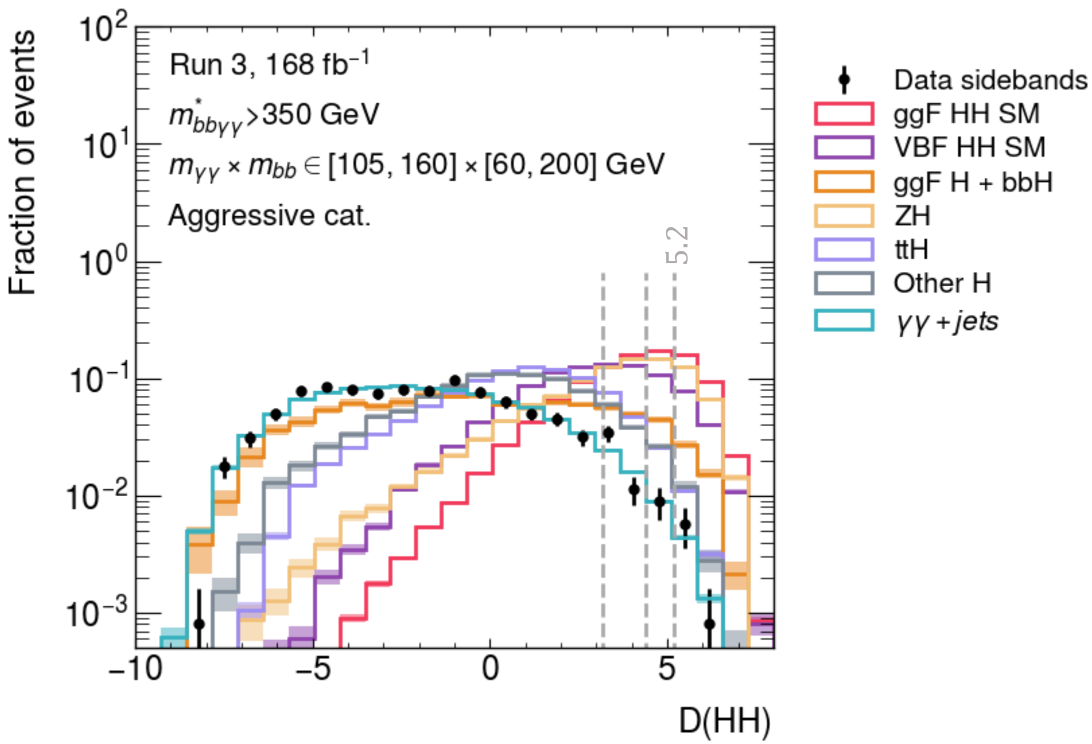

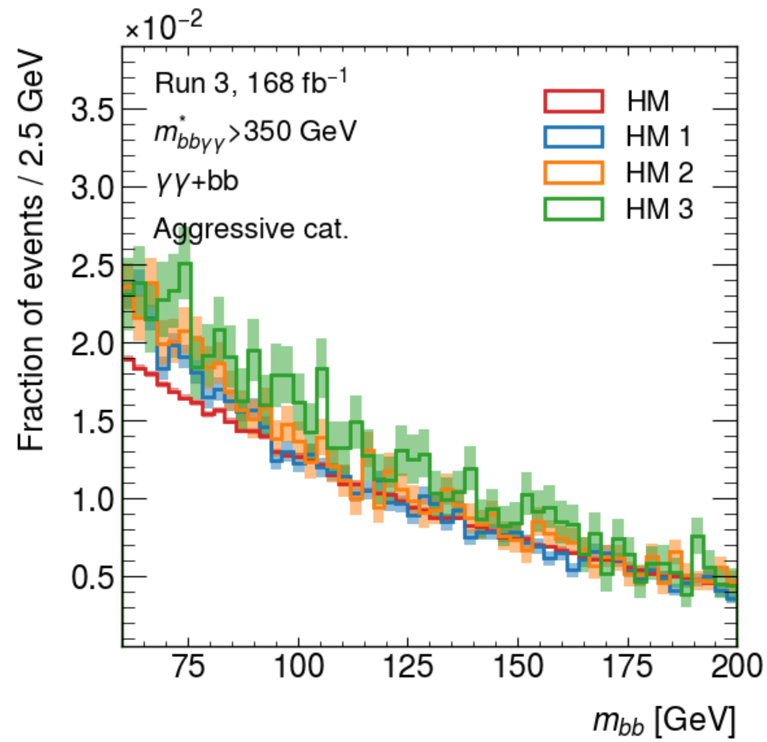

Successful decorrelation in m_{bb} after the categorisation

Categorisation Results: Counting Significance

Two-dimensional fit allows to exploit the granular information from both $m_{\gamma\gamma}$ and m_{bb}
→ Quantify how much the full m_{bb} granularity helps using binned counting significance:

$$Z_{\mathrm{bin}} = \sqrt{2 \cdot [(S+B) \cdot \log(1+S/B) - S]}, \quad Z_{\mathrm{total}} = \sqrt{\sum_{\mathrm{category}} \left(\sum_{\mathrm{bin}} Z_{\mathrm{bin}}^2 \right)}$$

Sum of Run 2 and Run 3 yields in $m_{\gamma\gamma} \in [120, 130]$ GeV and $m_{bb} \in [100, 150]$ GeV
S: HH yields ($\kappa_\lambda = 1$), B: Single Higgs + scaled $\gamma\gamma$+ jets yields

Binning	Bin width $m_{\gamma\gamma}$	Bin width m_{bb}	Z_{total}	
Single bin	–	–	0.994	
$m_{\gamma\gamma}$ binning	2 GeV	–	1.067	+7.3%
$m_{\gamma\gamma} \times m_{bb}$ binning	2 GeV	5 GeV	1.311	+22.9%

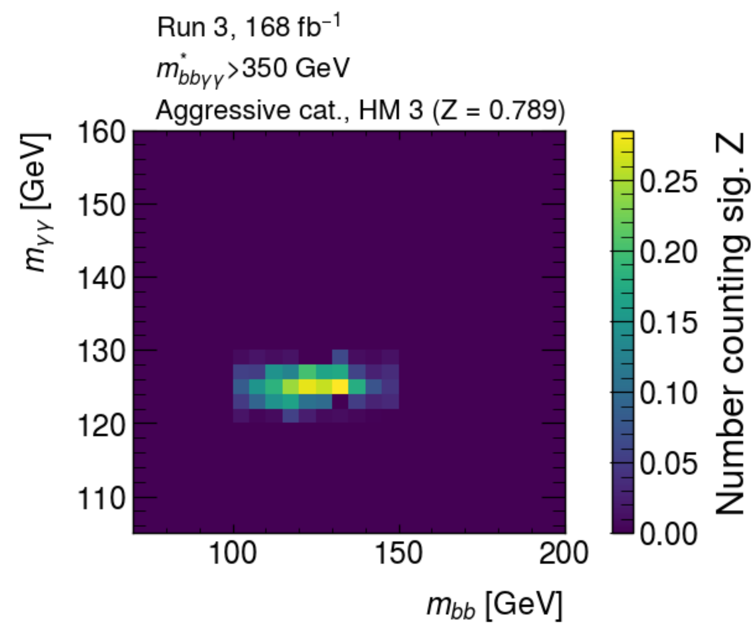

The two-dimensional $m_{\gamma\gamma} \times m_{bb}$ granularity helps discriminate against the background.

Modelling

Developed a dedicated modelling tool for signal & background shapes.

	$m_{\gamma\gamma}$	m_{bb}
HH	DSCB	DSCB
ZH	DSCB	DSCB
ggF H	DSCB	**Symbol Fit**
ttH	DSCB	**Symbol Fit**
Other H	DSCB	**Symbol Fit**
$\gamma\gamma$+jets	expo	expo

These single H processes have different shapes in each analysis category

The search for functions is done in each category via [SymbolFit] framework (based on symbolic regression)

- The search is done separately for ggF H and ttH processes
- Other H processes are merged and fitted together: bbH, $tHjb$, tWH, $VBFH$, $W^{\pm}H$

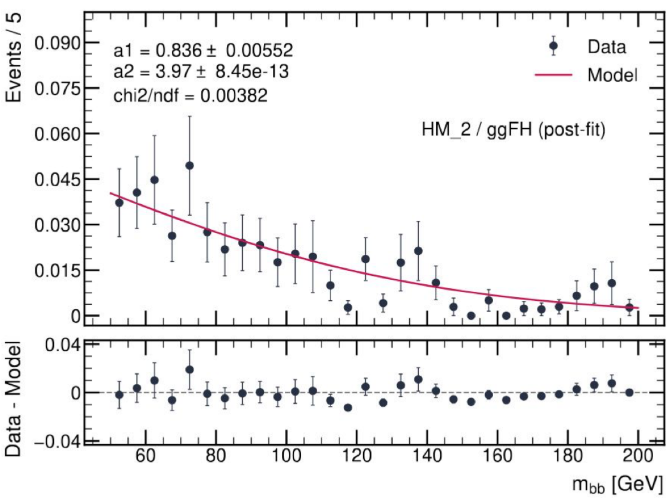

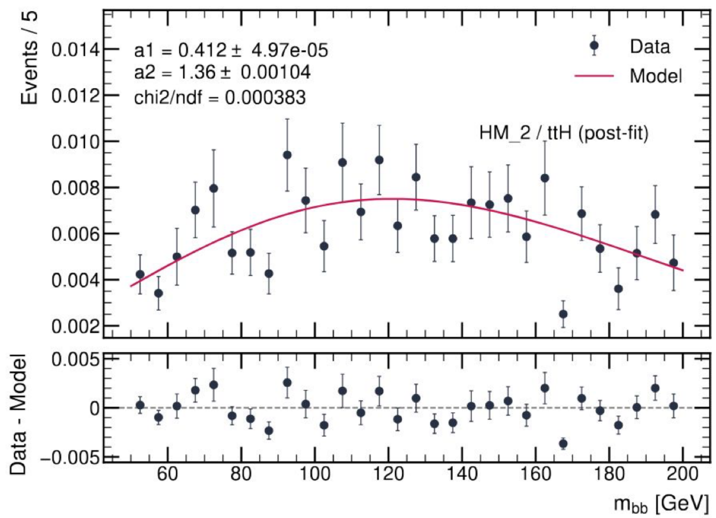

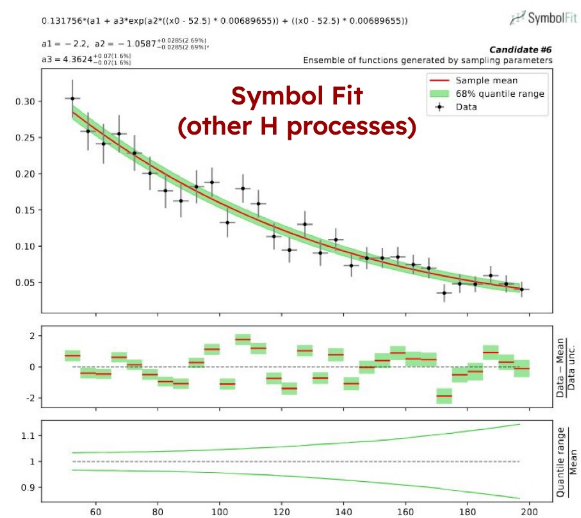

Data-driven Continuum BG Determination

Determine continuum BG shape and yield parameters by a side-band data $m_{\gamma\gamma} \times m_{bb}$ fit in each category with a blind region of $m_{\gamma\gamma} \in [120, 130]\mathrm{GeV}$.

Parameters in each category

	Run 2 ↔ Run3
Yield	Independent
Shape	Shared

Independent shape parameters can be selected depending on the categorisation strategy.

Run2HM_1

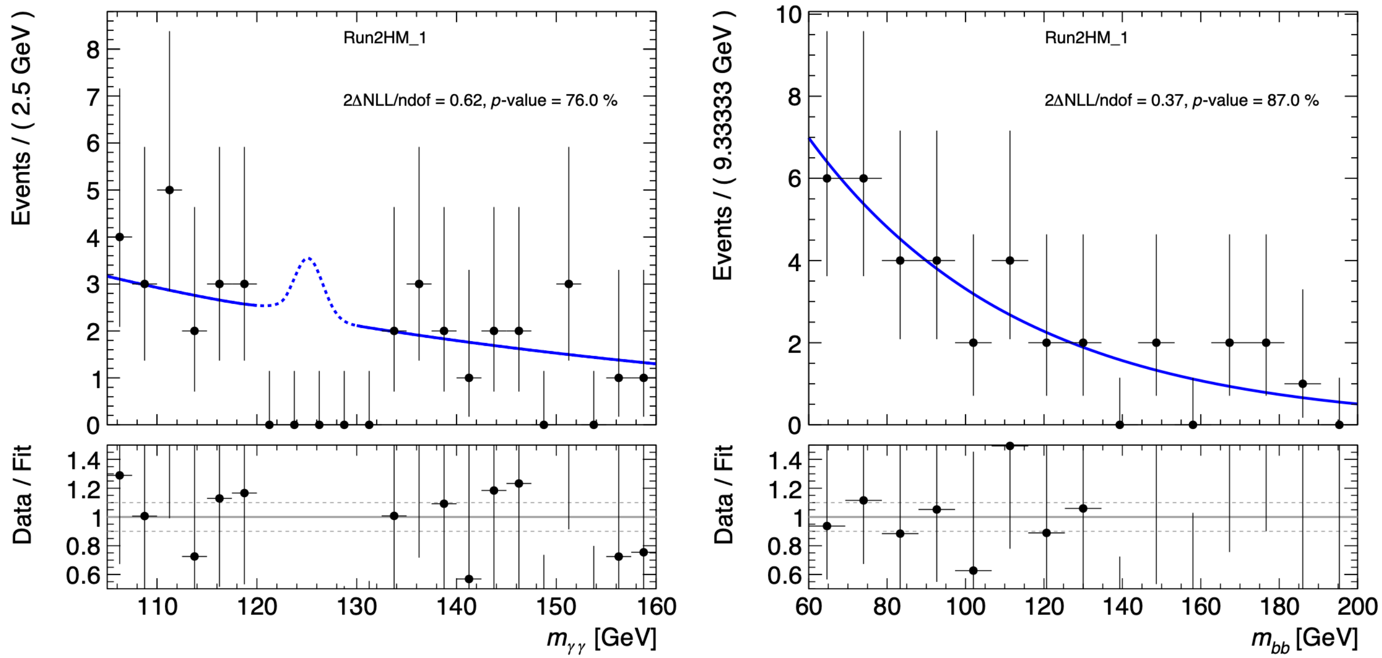

RooFit Workspace generation for unbinned 2D $m_{\gamma\gamma} \times m_{bb}$ fit via xmlAnaWSBuilder

Generate Asimov data set with data-driven continuum background components

Asimov Fit

Evaluated the μ_{HH} sensitivity using Asimov data corresponding to 308 and $423\ \mathrm{fb}^{-1}$.

HM ($m^*_{bb\gamma\gamma} > 350$ GeV)	2D $m_{\gamma\gamma}\times m_{bb}$ fit
LM ($m^*_{bb\gamma\gamma} \leqq 350$ GeV)	1D $m_{\gamma\gamma}$ fit

Combined

Categorisation by
different Transformer models

Run3HM_3

Post-fit pulls in 2D $m_{\gamma\gamma}\times m_{bb}$ distributions

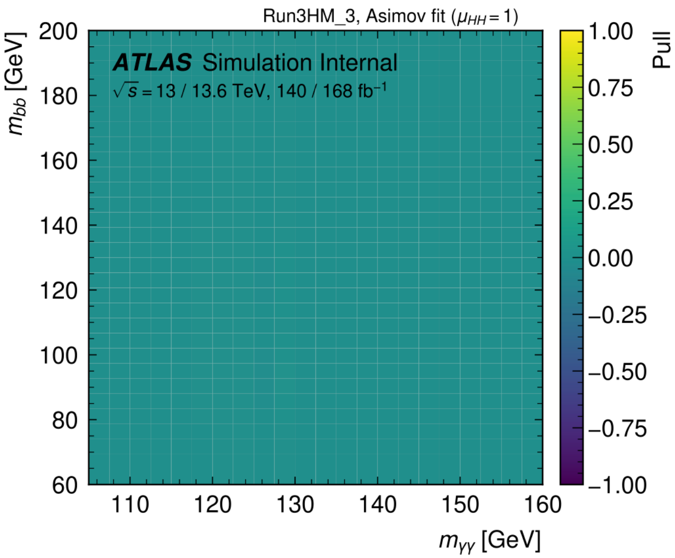

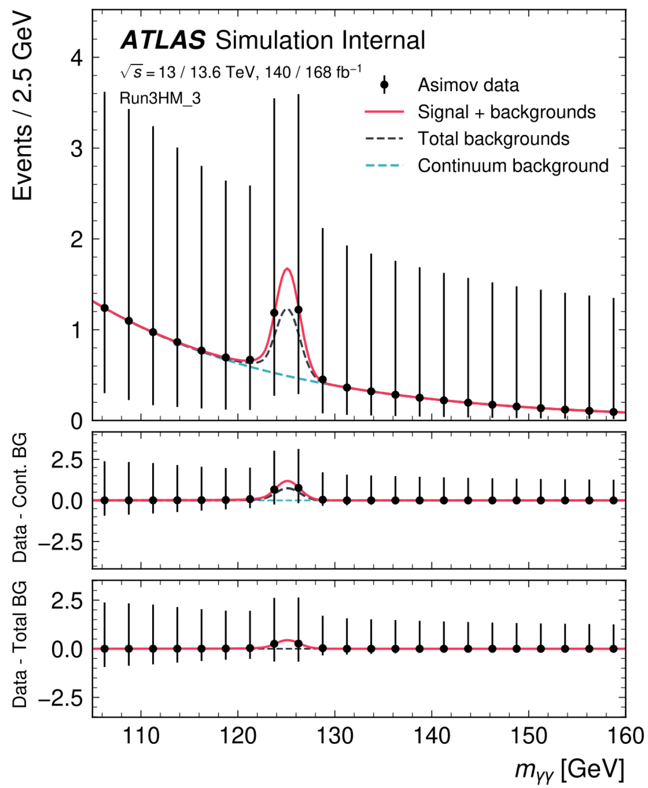

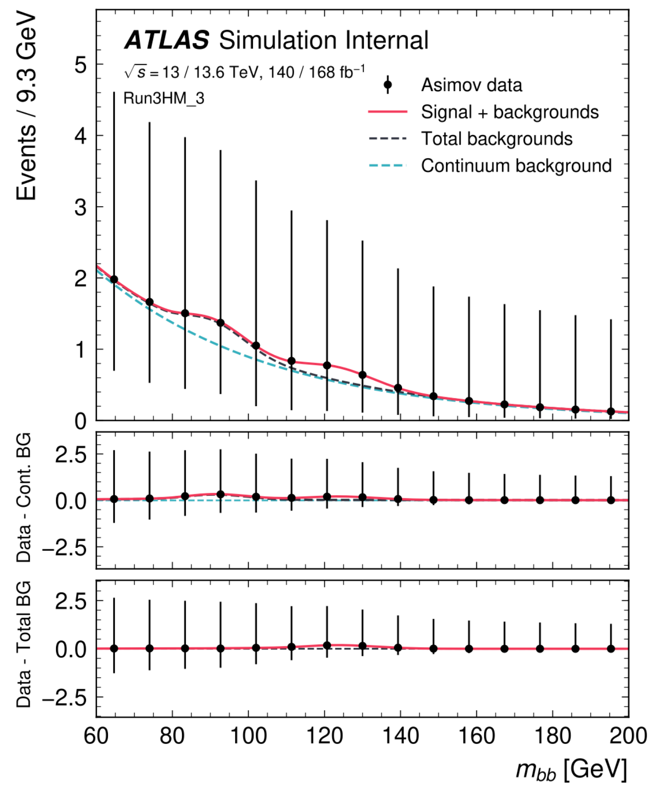

Healthy Asimov results observed

Stat-only μ_{HH} Sensitivity

Evaluated the μ_{HH} sensitivity using Asimov data corresponding to 308 and $423\ \mathrm{fb}^{-1}$.

	1D $m_{\gamma\gamma}$ fit Partial Run 3 HIGP-2025-10	$308\ \mathrm{fb}^{-1}$ (90%WP)		$423\ \mathrm{fb}^{-1}$ (90%WP)	
		1D fit	2D + 1D fit	1D fit	2D + 1D fit
Best fit	$1.000\ ^{+1.250}_{-0.936}$	$1.000\ ^{+1.205}_{-0.922}$	$1.000\ ^{+1.172}_{-0.824}$	$1.000\ ^{+1.011}_{-0.803}$	$1.000\ ^{+0.981}_{-0.729}$
Significance	1.083	1.104 $(+1.9\%)$	1.301 $(+20.1\%)$	1.297 $(+19.7\%)$	1.517 $(+40.0\%)$
Upper limit	2.287	2.191 (-4.2%)	2.064 (-9.7%)	1.795 (-21.5%)	1.675 (-26.8%)

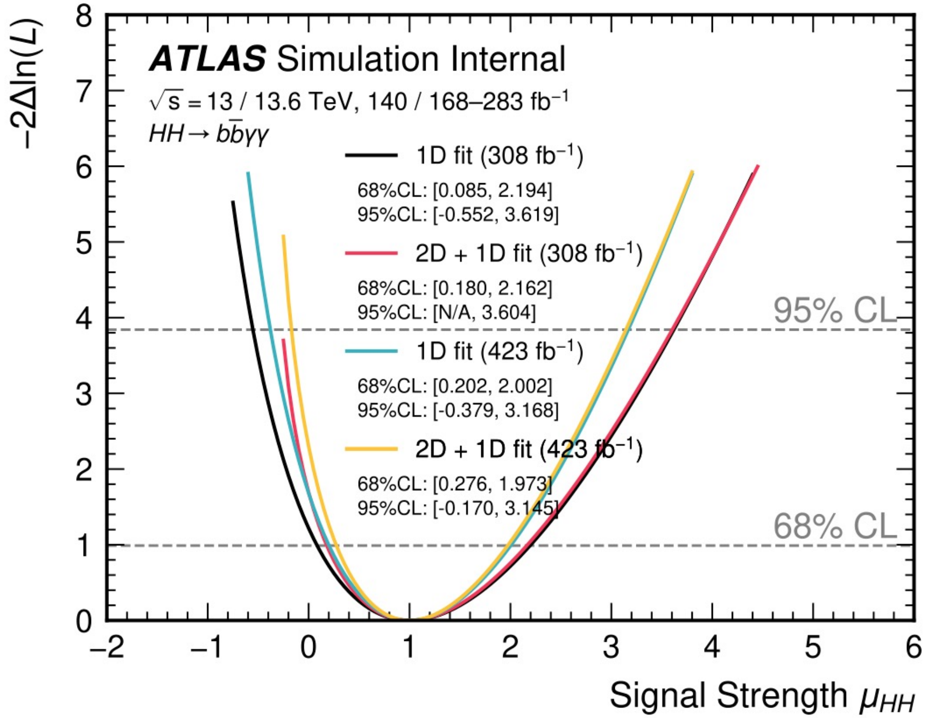

$423\ \mathrm{fb}^{-1}$
HH & ZH simultaneous fit (Other H fixed)
$\mu_{HH} = 1.000\ ^{+0.999}_{-0.740}$
$\mu_{ZH} = 1.000\ ^{+0.857}_{-0.675}$

Superior expected sensitivities!

Stat-only μ_{HH} Sensitivity with Unconditional μ_H

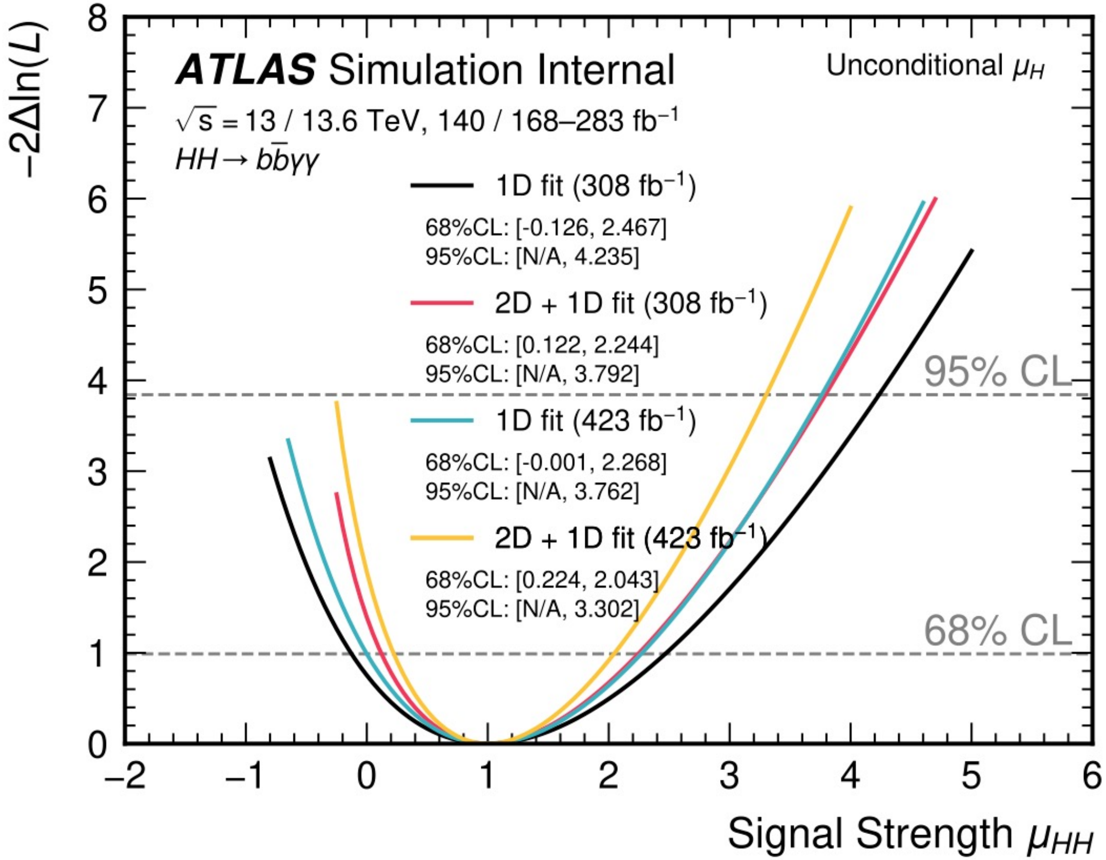

The 2D $m_{\gamma\gamma} \times m_{bb}$ fit shows more robustness against the single Higgs variations.

Stat-only κ_λ Sensitivity

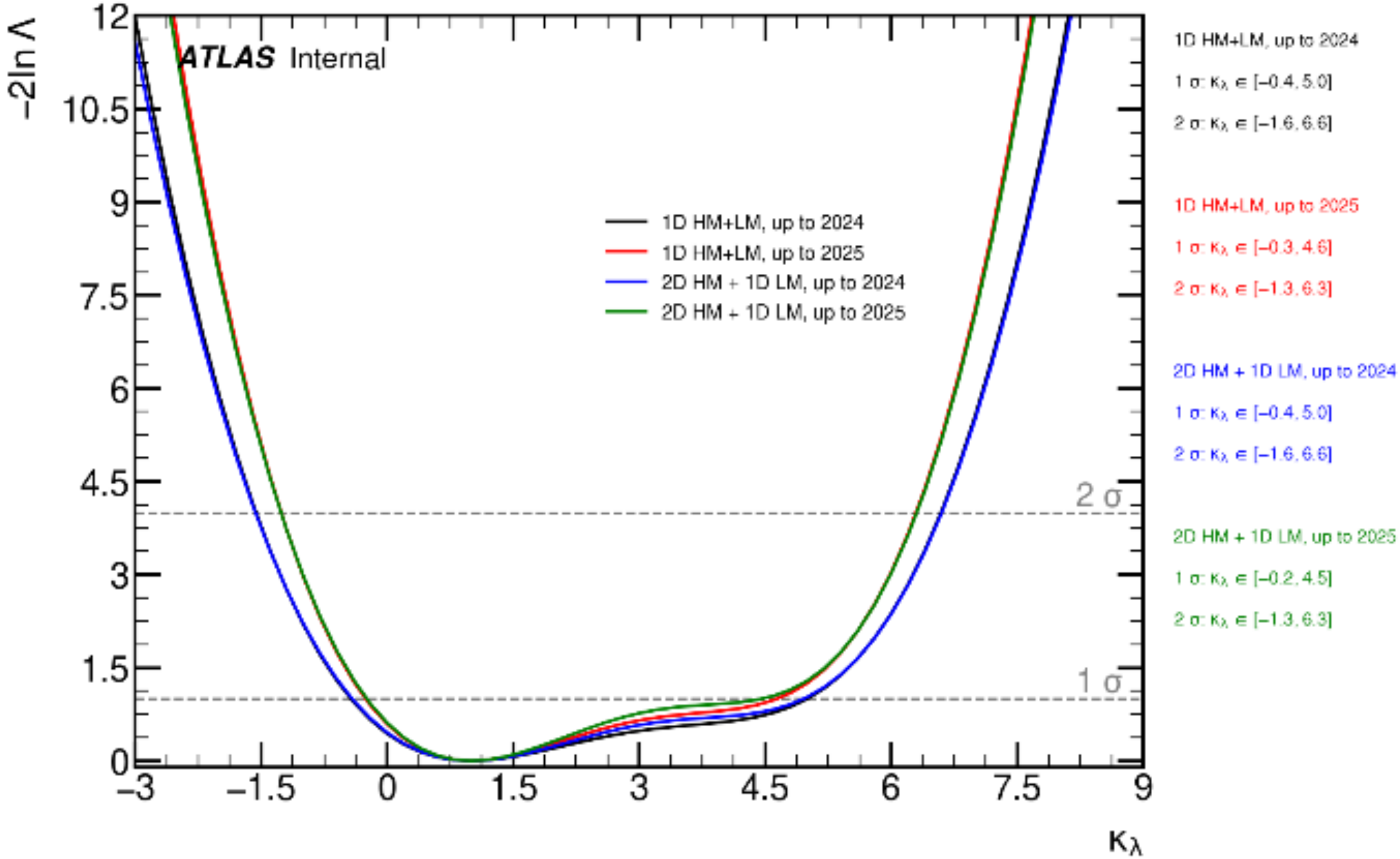

Comparable κ_λ sensitivity

Spurious Signal Results

Evaluated impact of spurious signals for 2D $m_{\gamma\gamma} \times m_{bb}$ fit by the following scan steps:

Peak position	Range	Step
$m_{\gamma\gamma}$	$[123.0, 127.0]$ GeV	0.5 GeV
m_{bb}	$[115.0, 135.0]$ GeV	2.0 GeV

Requirement

$$\max\left(\frac{N_{\mathrm{sp}}}{\sigma_{N_{bkg}}}\right) < 20\%$$

$S + B$ fit on $\gamma\gamma + bb$ samples with exponential functions

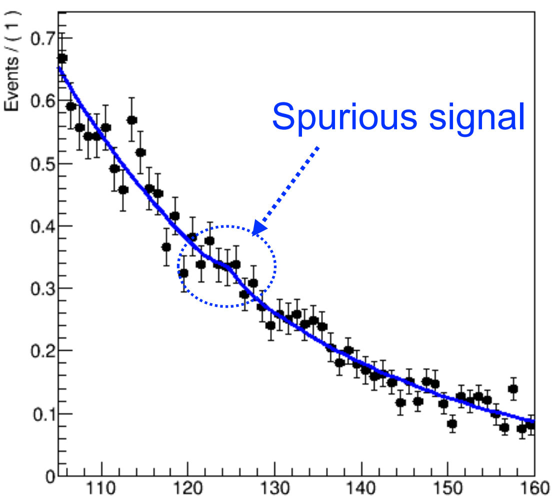

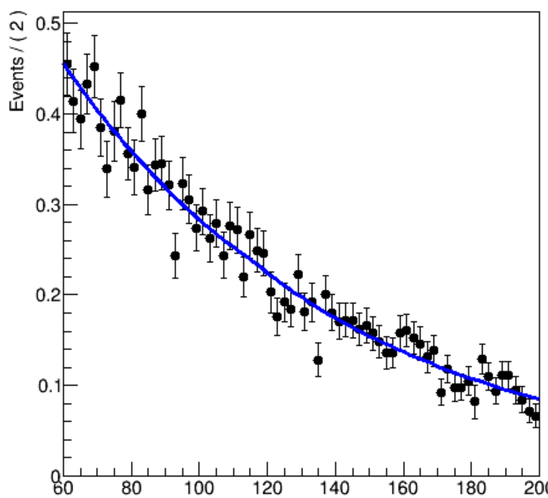

B-only fit on $\gamma\gamma + bb$ samples

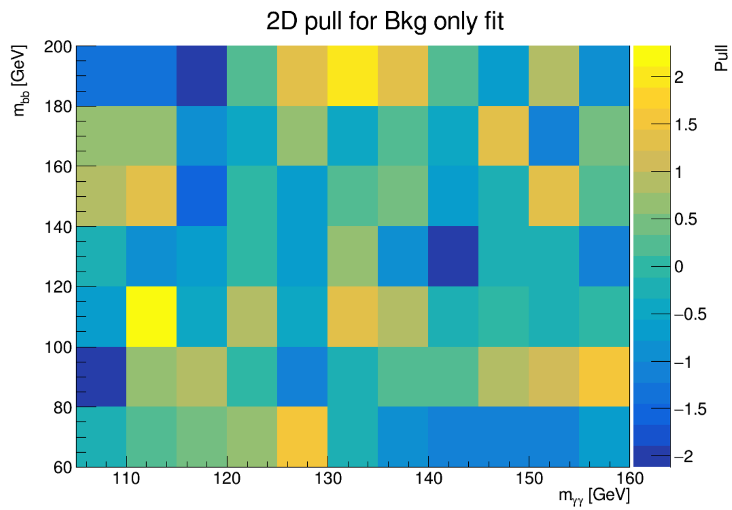

Take the maximum spurious signal as the uncertainty among various peak positions

Spurious Signal Results

Evaluated impact of spurious signals for 2D $m_{\gamma\gamma} \times m_{bb}$ fit by the following scan steps:

Peak position	Range	Step
$m_{\gamma\gamma}$	$[123.0, 127.0]$ GeV	0.5 GeV
m_{bb}	$[115.0, 135.0]$ GeV	2.0 GeV

Requirement

$$\max\left(\frac{N_{\text{sp}}}{\sigma_{N_{bkg}}}\right) < 20\%$$

All passed

Category	Expected HH yields	Spurious signal yields N_{sp}	$\max\left(\frac{N_{\text{sp}}}{\sigma_{N_{bkg}}}\right)$	BG-only fit Prob(χ^2)
HM 1	1.059	0.259	-4.83%	0.280
HM 2	0.821	-0.331	-0.26%	0.321
HM 3	1.069	0.0498	0%	0.426

With spurious signals*:
significance 1.194σ (-1.1%), upper limit 2.246 ($+0.4\%$) at $308\ \text{fb}^{-1}$

∗ Spurious signals for Run 2 + Run 3 categories assigned to each of the categories
→ Conservative estimation

Negligible impact from spurious signals

Summary

We have developed the 2D $m_{\gamma\gamma} \times m_{bb}$ fit method for the $HH \to b\bar{b}\gamma\gamma$ analysis.

- ✓ Successful m_{bb} decorrelation in a transformer model for the HM region
- ✓ Stat-only expected sensitivities by 2D fit (HM) + 1D fit (LM):
  $\sim 20\%(\sim 40\%)$ improvement in the μ_{HH} significance at $308(423)\ \mathrm{fb}^{-1}$ from 1D fit
- ✓ Negligible spurious signals in 2D $m_{\gamma\gamma} \times m_{bb}$ fit

Framework prepareation

Ready	2D $m_{\gamma\gamma} \times m_{bb}$ signal & background modelling [H+HH framework MR!14]
Ready	xmlAnaWSBuilder for 2D fits [xmlAnaWSBuilder MR!46]
Ongoing	XML generation for 2D $m_{\gamma\gamma} \times m_{bb}$ fit from YAML configs

Discussion

- ☐ m_{bb} fit range
- ☐ Requirement for continuum BG yields during categorisation

$HH \to b\bar{b}\gamma\gamma$ trigger development (relaxed photon ID with $m_{\gamma\gamma}$ & b-jet selections) slides

Appendix

Categorisation Requirements

Test two requirements for the minimum yields of continuum background during categorisation.

	Counting range	Scaled $\gamma\gamma$+jets simulation yields	
		Counting range	$m_{\gamma\gamma} \notin [120, 130]$ GeV
Conservative	$m_{\gamma\gamma} \in [130, 160]$ GeV $\cap$ $m_{bb} \in [125, 200]$ GeV	> 5 events	> 14 events ($m_{bb} \in [60, 200]$ GeV)
Aggressive	$m_{\gamma\gamma} \in [105, 160]$ GeV	> 11 events	> 9 events

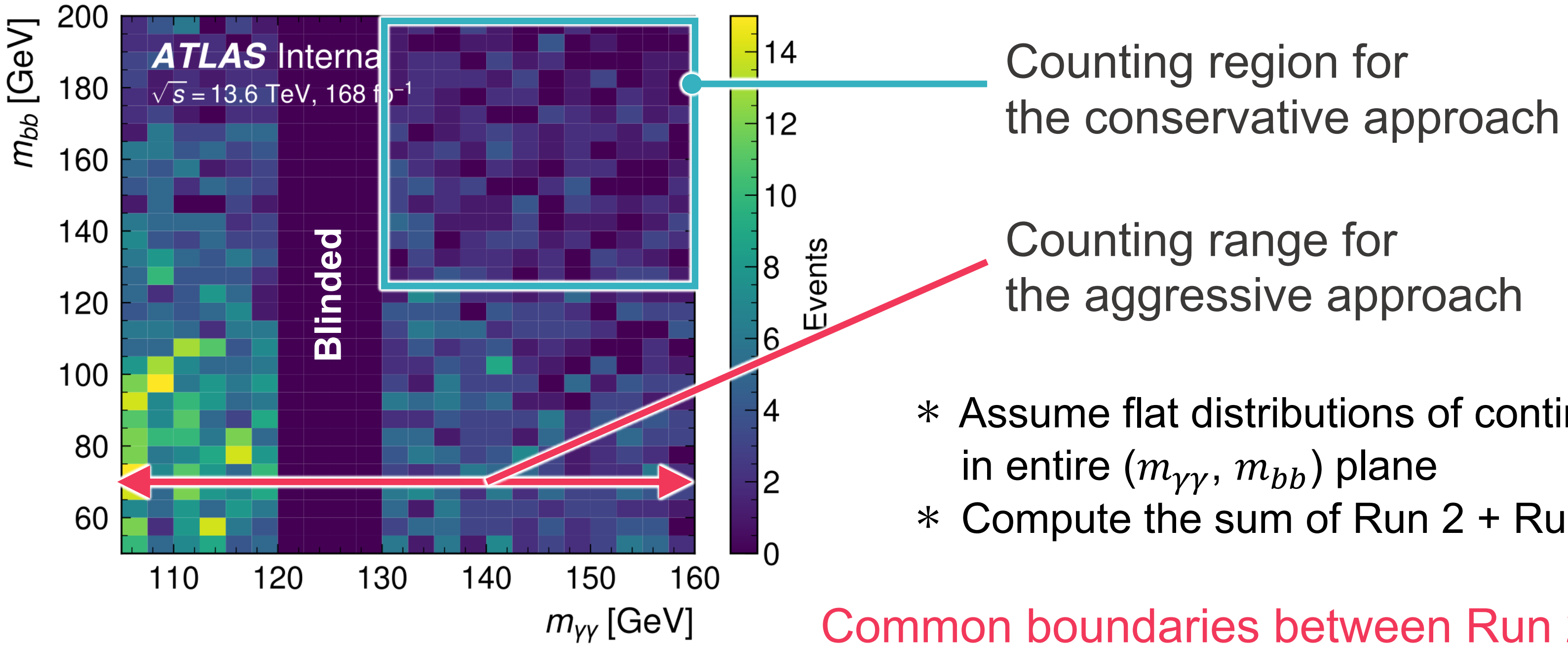

* Assume flat distributions of continuum BG in entire $(m_{\gamma\gamma}, m_{bb})$ plane
* Compute the sum of Run 2 + Run 3 yields

Common boundaries between Run 2 and Run 3

Categorisation Results: $D(HH)$

Set boundaries for **HM** categories:

- 3 categories for Run 2
- 3 categories for Run 3

Common boundaries

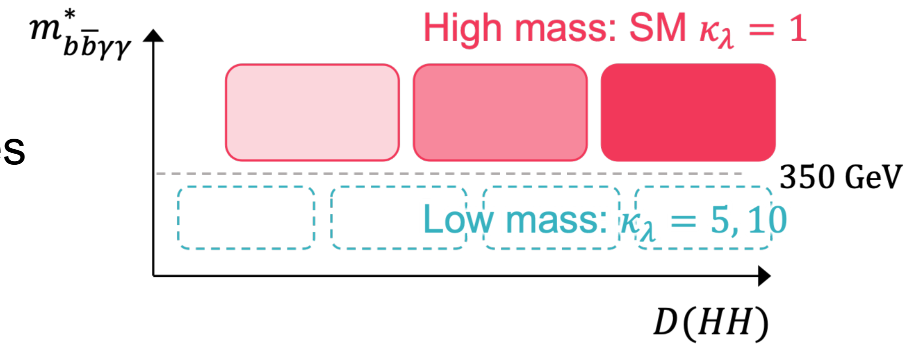

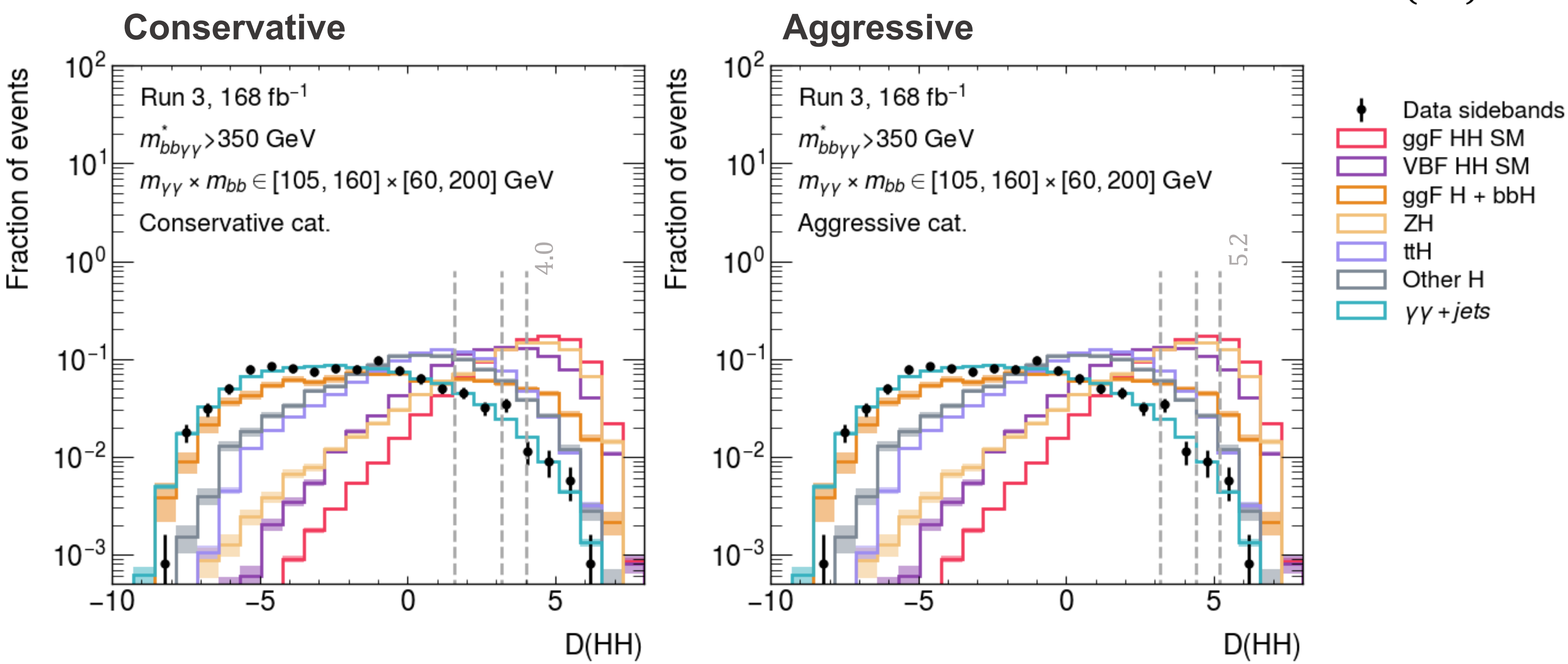

The aggressive approach allows tighter boundaries

Categorisation Results: $D(HH)$ — Run 2 vs Run 3

Test two requirements for the minimum yields of continuum background yields

Conservative

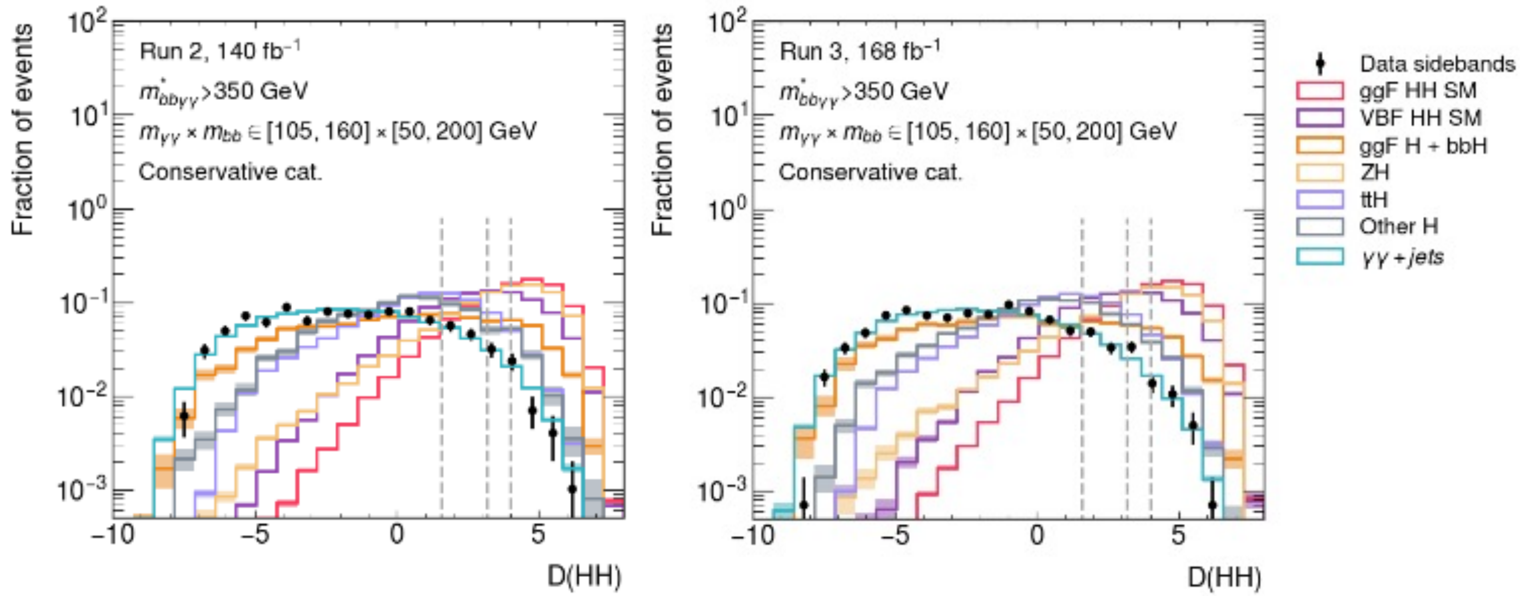

Aggressive

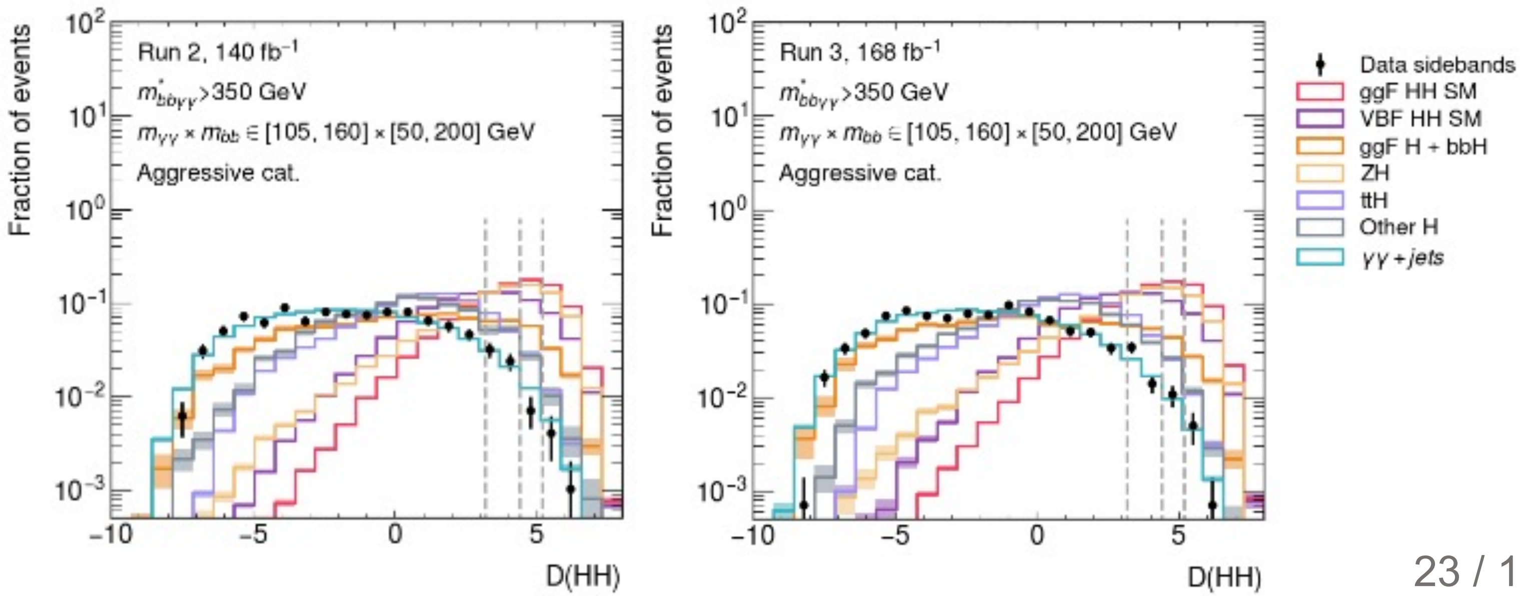

Categorisation Results: Counting Significance

Two-dimensional fit allows to exploit the granular information from both $m_{\gamma\gamma}$ and m_{bb}

→ Quantify how much the full m_{bb} granularity helps using binned counting significance:

$$Z_{\text{bin}} = \sqrt{2 \cdot [(S+B)\cdot \log(1+S/B) - S]}, \quad Z_{\text{total}} = \sqrt{\sum_{\text{category}} \left(\sum_{\text{bin}} Z_{\text{bin}}^2 \right)}$$

Sum of Run 2 and Run 3 yields in $m_{\gamma\gamma} \in [120, 130]$ GeV and $m_{bb} \in [100, 150]$ GeV

S: HH yields ($\kappa_\lambda = 1$), B: Single Higgs + scaled $\gamma\gamma$+ jets yields

Categorisation	Binning	Bin width $m_{\gamma\gamma}$	Bin width m_{bb}	Z_{total}	
Conservative	Single bin	–	–	0.894	
	$m_{\gamma\gamma}$ binning	2 GeV	–	0.975	+9.0%
	$m_{\gamma\gamma}\times m_{bb}$ binning	2 GeV	5 GeV	1.077	+10.5%
Aggressive	Single bin	–	–	0.994	
	$m_{\gamma\gamma}$ binning	2 GeV	–	1.067	+7.3%
	$m_{\gamma\gamma}\times m_{bb}$ binning	2 GeV	5 GeV	1.311	+22.9%

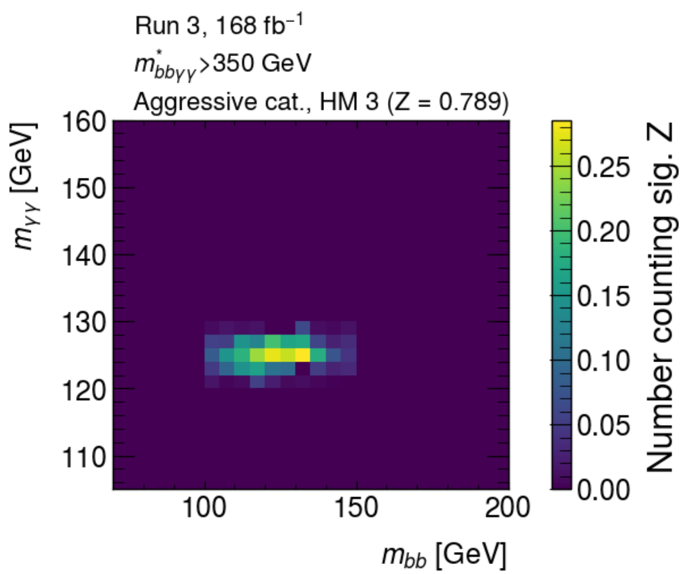

The two-dimensional$m\ \gamma\gamma\ \times\ m\ bb$ granularity helps discriminate against the background.

Decorrelation Check

Compared m_{bb} shapes in inclusive and categorised HM regions.

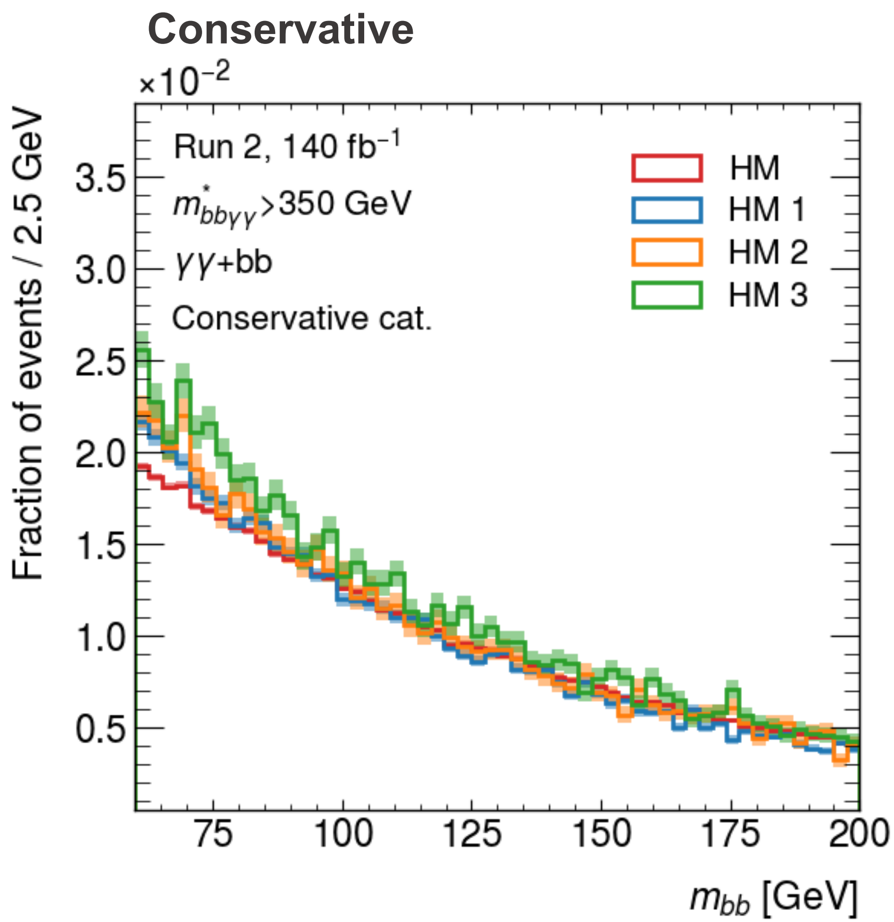

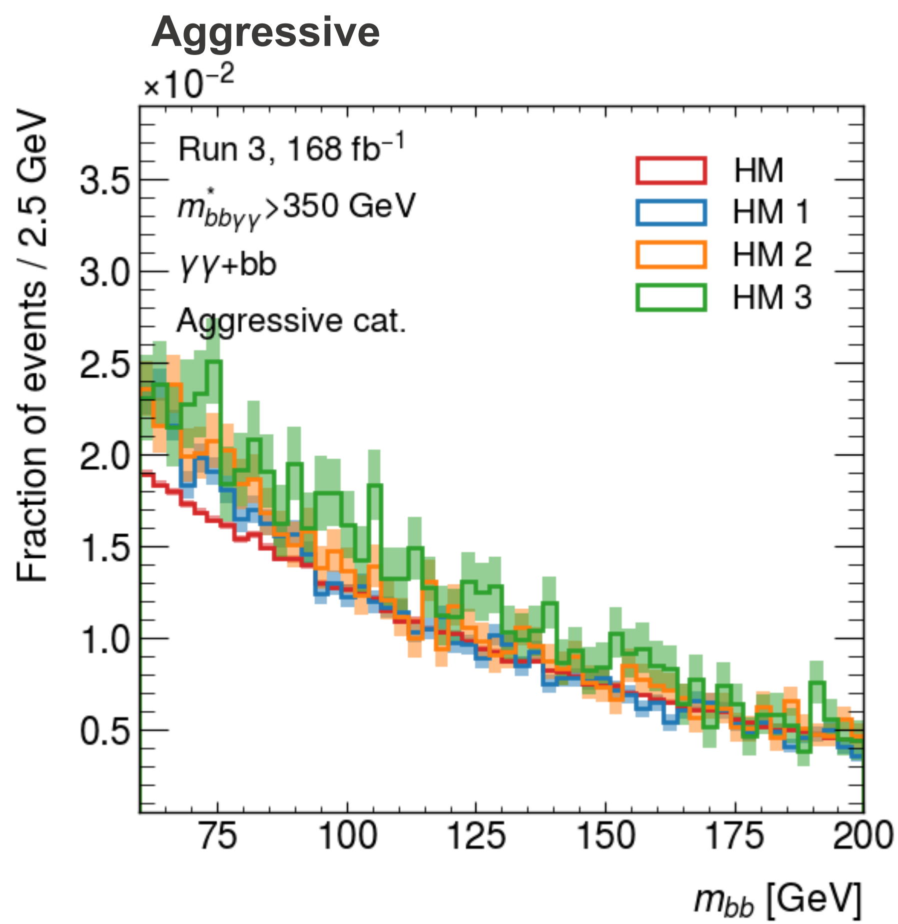

Signal-like structure inconspicuous in m_{bb}

Signal Modelling

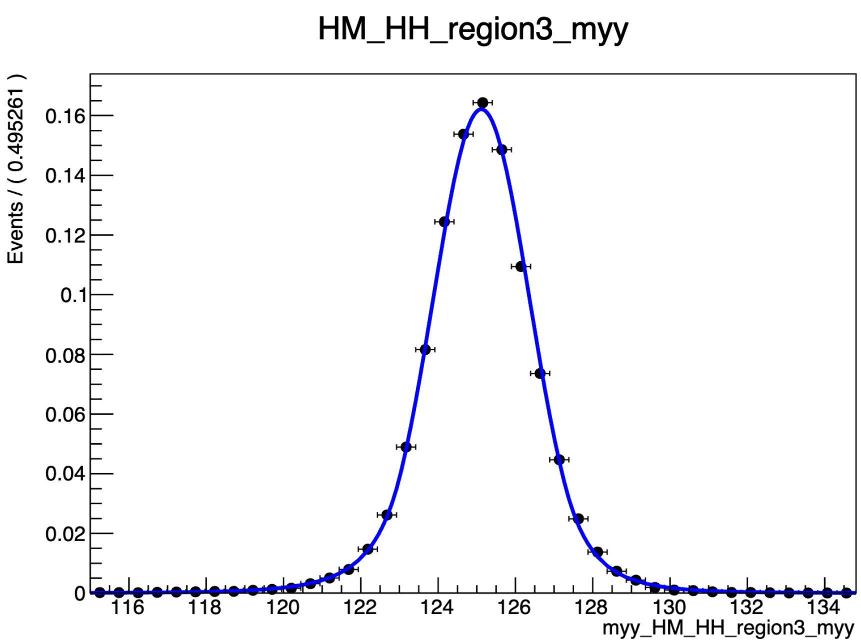

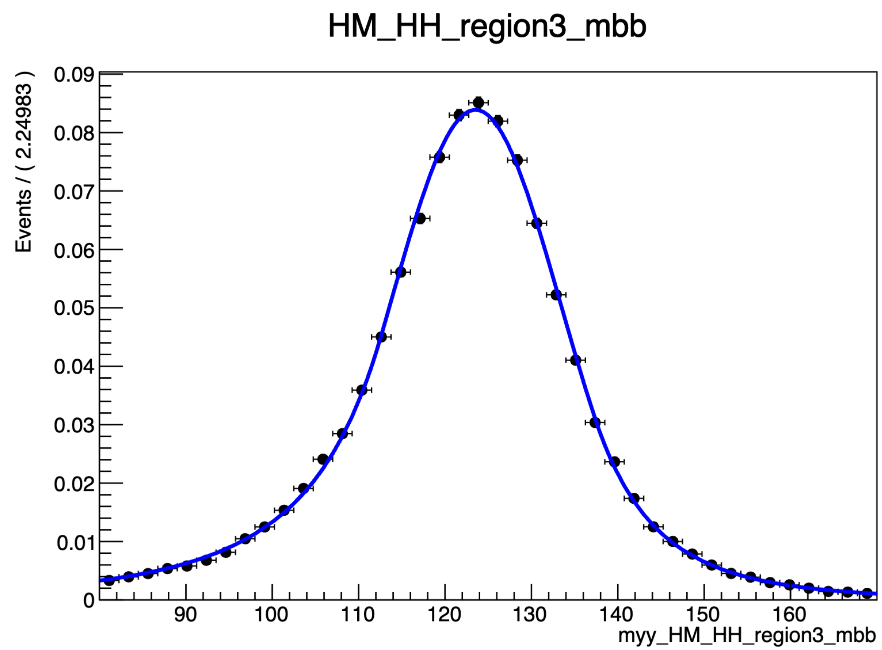

Stat-only μ_{HH} Sensitivity in HM

Evaluated the μ_{HH} sensitivity using Asimov data corresponding to 308 and $423\ \mathrm{fb}^{-1}$.

	1D $m_{\gamma\gamma}$ fit Partial Run 3 HIGP-2025-10	$308\ \mathrm{fb}^{-1}$ ($*$ HM only; 90%WP)		$423\ \mathrm{fb}^{-1}$ ($*$ HM only; 90%WP)	
		1D $m_{\gamma\gamma}$ fit	2D $m_{\gamma\gamma}\times m_{bb}$ fit	1D $m_{\gamma\gamma}$ fit	2D $m_{\gamma\gamma}\times m_{bb}$ fit
Best fit	$1.000^{+1.250}_{-0.936}$	$1.000^{+1.205}_{-0.922}$	$1.000^{+1.172}_{-0.824}$	$1.000^{+1.011}_{-0.803}$	$1.000^{+0.981}_{-0.729}$
Significance	1.083	1.102 $(+1.8\%)$	1.300 $(+20.0\%)$	1.295 $(+19.5\%)$	1.516 $(+39.9\%)$
Upper limit	2.287	2.200 (-3.8%)	2.069 (-9.5%)	1.799 (-21.3%)	1.678 (-26.6%)

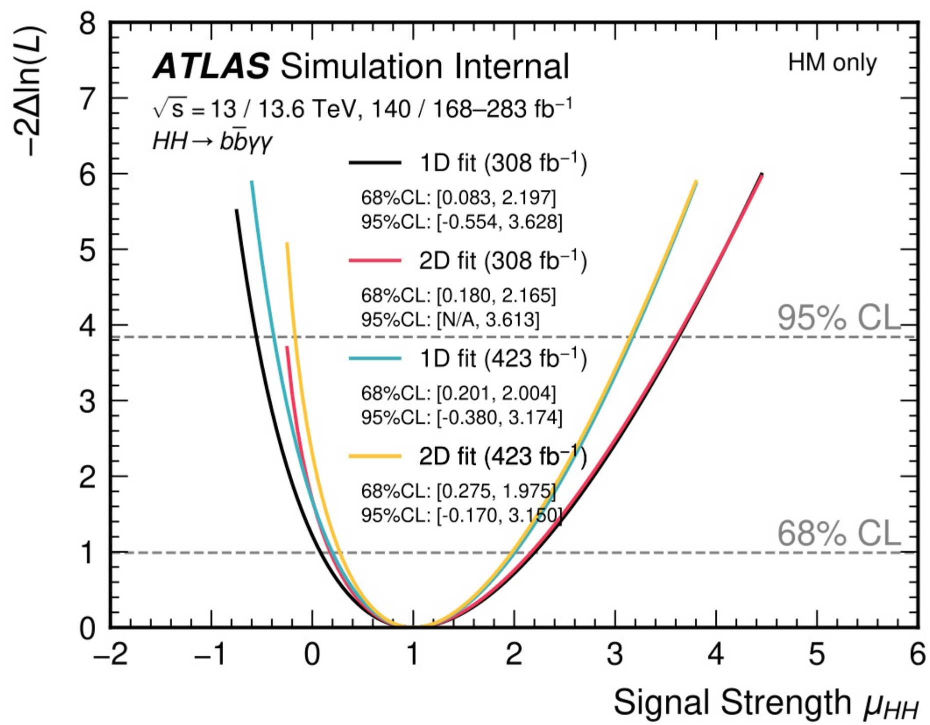

2D $m_{\gamma\gamma}\times m_{bb}$ Fit Results: Stat-only μ_{HH} Sensitivity

Evaluated the μ_{HH} sensitivity using Asimov data corresponding to $308\ \mathrm{fb}^{-1}$.

	1D $m_{\gamma\gamma}$ fit Partial Run 3 HIGP-2025-10	2D $m_{\gamma\gamma}\times m_{bb}$ fit (∗ HM only, 90%WP) Conservative	Aggressive
Best fit	$1.000\ ^{+1.250}_{-0.936}$	$1.000\ ^{+1.264}_{-0.941}$	$1.000\ ^{+1.246}_{-0.870}$
Significance	1.083	1.077 (-0.6%)	1.208 $(+11.5\%)$
Upper limit ($\mu_{HH}=0$)	2.287	2.329 $(+1.8\%)$	2.237 (-2.2%)

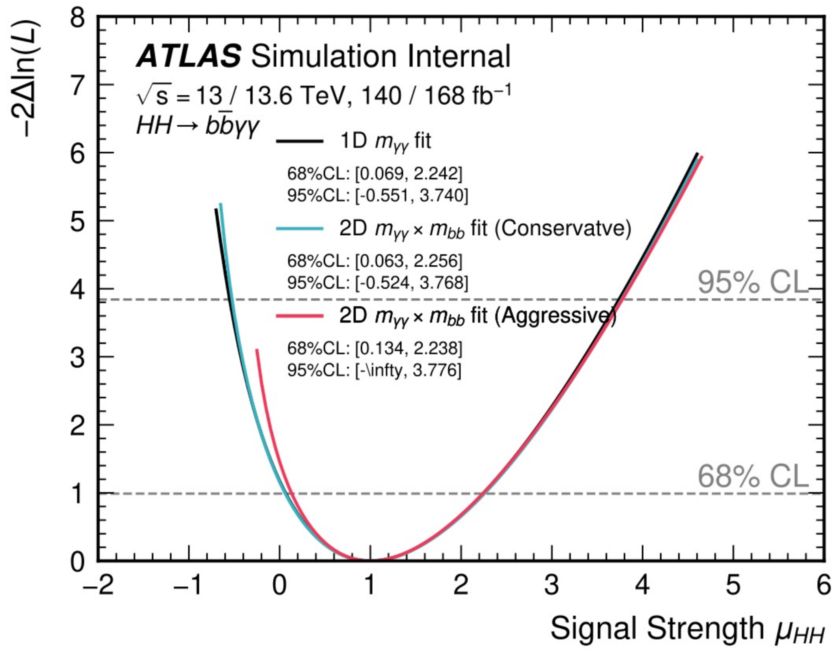

Aggressive categorisation

ZH sensitivities (HH fixed)

$$\mu_{ZH} = 1.000\ ^{+1.034}_{-0.783}$$

HH & ZH simultaneous fit

$$\mu_{HH} = 1.000\ ^{+1.270}_{-0.877}$$

$$\mu_{ZH} = 1.000\ ^{+1.046}_{-0.798}$$

$$\rho = -0.166$$

Superior expected sensitivity with the aggressive categorisations in HM

Stat-only μ_{HH} Sensitivity with Unconditional μ_H

Evaluated the μ_{HH} sensitivity under profiling single Higgs strength μ_H (without constraints).

	Profiling	1D $m_{\gamma\gamma}$ fit Partial Run 3 HIGP-2025-10	2D $m_{\gamma\gamma}\times m_{bb}$ fit (* HM only, 90%WP)	
			Conservative	Aggressive
Best fit μ_{HH}	μ_{HH}	$1.000^{+1.250}_{-0.936}$	$1.000^{+1.264}_{-0.941}$	$1.000^{+1.246}_{-0.870}$
	$\mu_{HH}+\mu_H$	$1.000^{+1.503}_{-1.174}$	$1.000^{+1.368}_{-1.016}$	$1.000^{+1.341}_{-0.927}$
μ_{HH} significance	μ_{HH}	1.083	1.077	1.208
	$\mu_{HH}+\mu_H$	0.835 (-22.9%)	0.981 (-8.9%)	1.107 (-8.4%)
Upper limit ($\mu_{HH}=0$)	μ_{HH}	2.287	2.329	2.237
	$\mu_{HH}+\mu_H$	2.751 ($+20.3\%$)	2.518 ($+8.1\%$)	2.404 ($+7.5\%$)

The 2D $m_{\gamma\gamma}\times m_{bb}$ fit shows more robustness against the single Higgs variations.

Stat-only κ_{2V} Sensitivity

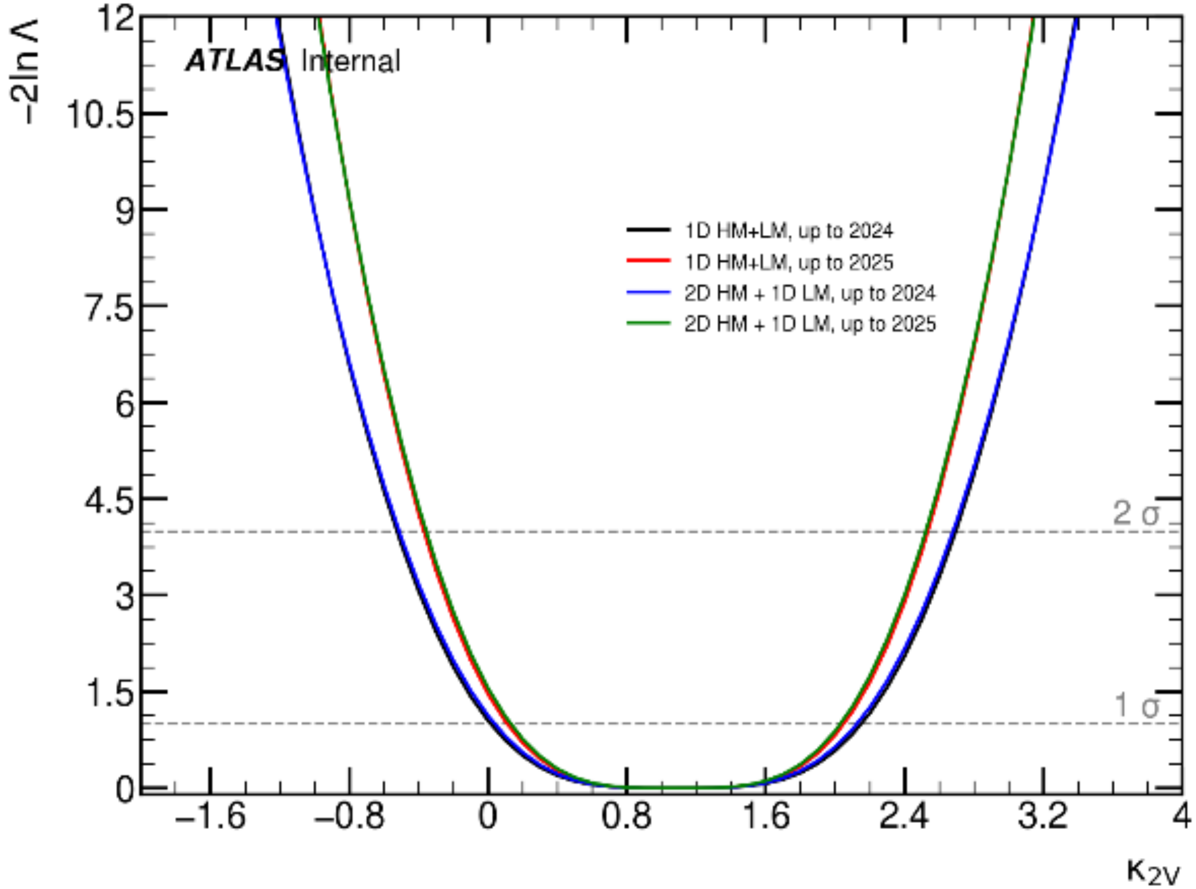

1D HM+LM, up to 2024
1 σ: $\kappa_{2V} \in [0.0, 2.2]$
2 σ: $\kappa_{2V} \in [-0.5, 2.7]$

1D HM+LM, up to 2025
1 σ: $\kappa_{2V} \in [0.1, 2.0]$
2 σ: $\kappa_{2V} \in [-0.4, 2.5]$

2D HM + 1D LM, up to 2024
1 σ: $\kappa_{2V} \in [0.0, 2.1]$
2 σ: $\kappa_{2V} \in [-0.5, 2.7]$

2D HM + 1D LM, up to 2025
1 σ: $\kappa_{2V} \in [0.1, 2.0]$
2 σ: $\kappa_{2V} \in [-0.4, 2.5]$

Comparable κ_λ sensitivity

Overestimation of Spurious Signal Uncertainty

The uncertainty of the spurious signals should be assigned to the total $\gamma\gamma$+jets yield in a category shared by Run 2 + Run 3 since the background shape is common between them.

$$\begin{array}{c} N_{\gamma\gamma+\text{jets}}^{\text{Run 2}} \\ + \\ N_{\gamma\gamma+\text{jets}}^{\text{Run 3}} \end{array} \cdot p_{\gamma\gamma+\text{jets}}^{\text{Run 2+Run 3}}\left(x;\vec{\theta}_{\gamma\gamma+\text{jets}}\right) + N_{\text{SS}}^{\text{Run 2+Run 3}} \cdot p_{HH}(x;\theta_{\text{SS}})$$

However, the current implementation via xmlAnaWSbuilder assigns the spurious signal uncertainty to each $\gamma\gamma$+jets yield of Run 2 and Run 3.

$$N_{\gamma\gamma+\text{jets}}^{\text{Run 2}} \cdot p_{\gamma\gamma+\text{jets}}^{\text{Run 2+Run 3}}\left(x;\vec{\theta}_{\gamma\gamma+\text{jets}}\right) + N_{\text{SS}}^{\text{Run 2+Run 3}} \cdot p_{HH}(x;\theta_{\text{SS}})$$

$$N_{\gamma\gamma+\text{jets}}^{\text{Run 3}} \cdot p_{\gamma\gamma+\text{jets}}^{\text{Run 2+Run 3}}\left(x;\vec{\theta}_{\gamma\gamma+\text{jets}}\right) + N_{\text{SS}}^{\text{Run 2+Run 3}} \cdot p_{HH}(x;\theta_{\text{SS}})$$

Double counting

∗ The (background) PDF shape parameters $\vec{\theta}_{\gamma\gamma+\text{jets}}$ are still shared between Run 2 and Run 3.

Roughly twice larger spurious signals are allowed…

Run 2: $\dfrac{308}{140} \sim 2.2$ Run 3: $\dfrac{308}{168} \sim 1.8$

∗ Not taken into account scale factor differences between Run 2 and Run 3

Significant degradation in the 2D $m_{\gamma\gamma} \times m_{bb}$ fit could be induced by this overestimation.

Run-dep. Assignments of Spurious Signal Uncertainty

The spurious signal uncertainty is distributed according to the expected $\gamma\gamma$+jets yield fractions, using scaled simulation, in each of the Run 2 and Run 3 categories.

Gaussian constraints for spurious signals

	Inclusive σ $\gamma\gamma + bb$ `public_test`	Inclusive σ Full $\gamma\gamma + bb$		Run-dep. σ	Scaled $\gamma\gamma$+jets yield	Fraction	SF $m_{\gamma\gamma} \notin [120, 130]$ GeV
HM_1	0.292	0.269	Run 2	0.133	151.94	49.4%	1.864
			Run 3	0.136	155.38	50.6%	1.417
HM_2	0.330	0.194	Run 2	0.0832	48.75	42.8%	1.726
			Run 3	0.1108	64.97	57.1%	1.898
HM_3	0.268	0.102	Run 2	0.0406	18.93	39.8%	1.133
			Run 3	0.0614	28.58	60.2%	1.265

(cf) The luminosity fraction: Run 2 = 45.5%, Run3 = 54.5%

⚠ While this split assignment serves as a reasonable approximation, simply dividing the inclusive spurious signal from a merged category could overlook potential Run-dependent shape deviations.

Spurious Signal Impacts

Correlate the nuisance parameter in corresponding categories from both Run 2 and Run 3.

$$N_{\gamma\gamma+\text{jets}}^{\text{Run 2}} \cdot p_{\gamma\gamma+\text{jets}}^{\text{Run 2+Run 3}}(x; \vec{\theta}_{\gamma\gamma+\text{jets}}) + N_{\text{SS}}^{\text{Run 2}} \cdot p_{HH}(x; \theta_{\text{SS}})$$

$$N_{\gamma\gamma+\text{jets}}^{\text{Run 3}} \cdot p_{\gamma\gamma+\text{jets}}^{\text{Run 2+Run 3}}(x; \vec{\theta}_{\gamma\gamma+\text{jets}}) + N_{\text{SS}}^{\text{Run 3}} \cdot p_{HH}(x; \theta_{\text{SS}})$$

Shared

Two scenarios are tested for assigned uncertainty magnitudes

Inclusive SS	$N_{\text{SS}}^{\text{Run 2+Run 3}} = N_{\text{SS}}^{\text{Run 2}} = N_{\text{SS}}^{\text{Run 3}}$
Split SS	$N_{\text{SS}}^{\text{Run 2+Run 3}} = N_{\text{SS}}^{\text{Run 2}} + N_{\text{SS}}^{\text{Run 3}}$

Split based on the $\gamma\gamma$+jets yield fractions

	Stat-only	With inclusive SS $\gamma\gamma + bb$ `public_test`	With inclusive SS Full $\gamma\gamma + bb$	With split SS Full $\gamma\gamma + bb$
Best fit	$1.000^{+1.244}_{-0.893}$	$1.000^{+1.278}_{-0.953}$	$1.000^{+1.247}_{-0.900}$	$1.000^{+1.244}_{-0.895}$
Significance	1.157	1.060 (-8.3%)	1.145 (-1.0%)	1.154 (-0.3%)
Upper limit ($\mu_{HH} = 0$)	2.258	2.339 $(+3.6\%)$	2.264 $(+0.3\%)$	2.259 $(+0.0\%)$

The spurious signal impacts are controlled below 1%.

Their impacts are negligible with spurious signal uncertainty split.

Possible Strategy for Spurious Signals

	Method	$\sigma(\mu_{HH})$
1	Allow doubled spurious signals	$\sim 1.0\%$
2	Distribute spurious signal uncertainties based on yields The shape agreements between Run 2 and Run 3 should be verified: e.g. Kolmogorov-Smirnov tests.	$\sim 0.3\%$
3	Estimate spurious signals using simultaneous fits in separate Run 2 and Run 3 categories	$\sim 0.3\%$?

Figure: Categorization